Anal. Chem. **2010,** *82,* 9528–9533

Bioimaging of Metals and Biomolecules in Mouse Heart by Laser Ablation Inductively Coupled Plasma Mass Spectrometry and Secondary Ion Mass Spectrometry

J. Sabine Becker,*,† Uwe Breuer,† Hui-Fang Hsieh,† Tobias Osterholt,‡ Usarat Kumtabtim,† Bei Wu,† Andreas Matusch,‡ Joseph A. Caruso,|| and Zhenyu Qin§

Central Division of Analytical Chemistry and Institute of Neurosciences and Medicine (INM-1 and -2), Forschungszentrum Jülich, D-52425 Jülich, Germany, and Division of Cardiovascular Disease, College of Medicine, and Department of Chemistry, University of Cincinnati, Cincinnati, Ohio, United States

Bioimaging mass spectrometric techniques allow direct mapping of metal and biomolecule distributions with high spatial resolution in biological tissue. In this study laser ablation inductively coupled plasma mass spectrometry (LA-ICPMS) was used for imaging of transition metals (Fe, Cu, Zn, Mn, and Ti), alkali and alkaline-earth metals (Na, K, Mg, and Ca, respectively), and selected nonmetals (such as C, P, and S) in native cryosections of mouse heart. The metal and nonmetal images clearly illustrated the shape and the anatomy of the samples. Zinc and copper were inhomogeneously distributed with average concentrations of 26 and 11 $\mu g\ g^{-1}$, respectively. Titanium and manganese were detected at concentrations reaching 1 and 2 $\mu g\ g^{-1}$, respectively. The highest regional metal concentration of 360 $\mu g\ g^{-1}$was observed for iron in blood present in the lumen of the aorta. Secondary ion mass spectrometry (SIMS) as an elemental and biomolecular mass spectrometric technique was employed for imaging of Na, K, and selected biomolecules (e.g., phosphocholine, choline, cholesterol) in adjacent sections. Here, two different bioimaging techniques, LA-ICPMS and SIMS, were combined for the first time, yielding novel information on both elemental and biomolecular distributions.

Bioimaging analytical techniques are today of key interest in life science studies and have been rapidly growing in biology and medicine.[1−4] Different non mass spectrometric bioimaging techniques, such as scanning electron microscopy with energy-dispersive X-ray analysis (SEM−EDX),[5] energy-filtering transmission electron microscopy (EFTEM),[6] proton-induced X-ray emission (PIXE),[7] or micro and nano X-ray fluorescence (nanoXRF), e.g., using a synchrotron radiation facility,[8] Raman spectrometry, a plethora of fluorescence microscopic techniques,[9] and all the armory of labeling and detection techniques using reactions in situ, have been established and employed to visualize structures to study elemental and molecular distributions in biological tissues ex vivo. These are complemented in vivo by fluorescence−optical techniques, positron emission tomography (PET),[10,11] and nuclear magnetic resonance imaging (MRI).

In the past few years mass spectrometric analytical methods such as matrix-assisted laser desorption/ionization mass spectrometry (MALDI-MS),[12−19] desorption electrospray ionization mass spectrometry (DESI),[20] or secondary ion mass spectrometry (SIMS) have been widely applied for imaging and mapping of

* To whom correspondence should be addressed. Phone: +49 2461612698. Fax: +49 2461612560. E-mail: s.becker@fz-juelich.de.

† Central Division of Analytical Chemistry, Forschungszentrum Jülich.

‡ Institute of Neurosciences and Medicine (INM-1 and -2), Forschungszentrum Jülich.

§ Division of Cardiovascular Disease, College of Medicine, University of Cincinnati.

|| Department of Chemistry, University of Cincinnati.

(1) Rubakhin, S. S., Sweedler, J. V., Eds. *Mass Spectrometric Imaging: Principles and Protocols*; Methods in Molecular Biology 656; Springer: Heidelberg, Germany, September 2010.

(2) Becker, J. S.; Zoriy, M.; Matusch, A.; Wu, B.; Salber, D.; Palm, C.; Becker, J. Su. *Mass Spectrom. Rev.* **2010**, *29*, 156.

(3) Matusch, A.; Depboylu, C.; Palm, C.; Wu, B.; Höglinger, G. U.; Schäfer, M. K.-H.; Becker, J. S. *J. Am. Soc. Mass Spectrom.* **2010**, *21*, 161.

(4) Becker, J. S. *Int. J. Mass Spectrom.* **2010**, *289*, 65.

(5) Zvyagin, A. V.; Zhao, X.; Gierden, A.; Sanchez, W.; Ross, J. A.; Roberts, M. S. *J. Biomed. Opt.* **2008**, *13*, 064031.

(6) Reimer, L.; Kohl, H. *Transmission Electron Spectroscopy: Physics of Image Formation*; Springer: New York, 2008.

(7) Rajendran, R.; Minqin, R.; YNsa, M. D.; Casadesus, G.; Smith, M. A.; Perry, G.; Halliwell, B.; Watt, F. *Biochem. Biophys. Res. Commun.* **2009**, *382*, 91.

(8) Carmona, A.; Cloetens, P.; Devès, G.; Bohic, S.; Ortega, R. *J. Anal. At. Spectrom.* **2008**, *23*, 1083.

(9) Rao, M. S.; Hattiangadya, B.; Shetty, A. K. *Neurobiol. Dis.* **2006**, *21*, 276.

(10) Wahl, R. L.; Zasadny, K.; Helvie, M.; Hutchins, G. D.; Weber, B.; Cody, R. *J. Clin. Oncol.* **1993**, *11*, 2101.

(11) Langen, K.-J.; Salber, D.; Hamacher, H.; Stoffels, G.; Reifenberger, G.; Pauleit, D.; Coenen, H.; Zilles, K. *J. Nucl. Med.* **2007**, *48*, 1482.

(12) Stoeckli, M.; Chaurand, P.; Hallahan, D. E.; Caprioli, R. M. *Nat. Med.* **2001**, *7*, 493.

(13) Grey, A. C.; Gelasco, A. K.; Section, J.; Moreno-Rodriguez, R. A.; Krug, E. L.; Schey, K. L. *Anat. Rec.* **2010**, *293*, 821.

(14) Caprioli, R. M.; Farmer, T. B.; Gile, J. *Anal. Chem.* **1997**, *69*, 4751.

(15) Cornett, D. S.; Frappier, S. L.; Caprioli, R. M. *Anal. Chem.* **2008**, *80*, 5648.

(16) Seeley, E. H.; Oppenheimer, S. R.; Mi, D.; Chaurand, P.; Caprioli, R. M. *J. Am. Soc. Mass Spectrom.* **2008**, *19*, 1069.

(17) McLean, J. A.; Ridenour, W. B.; Caprioli, R. M. *J. Mass Spectrom.* **2007**, *42*, 1099.

(18) Norris, J. L.; Cornett, D. S.; Mobley, J. A.; Andersson, M.; Seeley, E. H.; Chaurand, P.; Caprioli, R. M. *Int. J. Mass Spectrom.* **2007**, *260*, 212.

(19) Chaurand, P.; Cornett, D. S.; Caprioli, R. M. *Curr. Opin. Biotechnol.* **2006**, *17*, 431.

(20) Girod, M.; Shi, Y.; Chen, J. X.; Cooks, R. G. *J. Am. Soc. Mass Spectrom.* **2010**, *21*, 1177.

10.1021/ac102256q
Published on Web 10/26/2010

biomolecules and elements or identifying specific compounds.[21−28] SIMS allows imaging at submicrometer lateral resolution. All these mass spectrometric techniques are being further developed and applied for imaging studies of biological systems to provide information on various classes of biomolecules (such as proteins, metabolites, and lipids) and metals with lateral resolution at the micrometer scale.

Recently, LA-ICPMS (laser ablation inductively coupled plasma mass spectrometry) as elemental mass spectrometry has been developed for bioimaging of trace metals, especially for the essential transition metals Fe, Cu, and Zn, and of selected nonmetals (such as C, P, and S). LA-ICPMS uses a laser beam to evaporate sample material in an argon atmosphere under normal pressure. The ablated material is then transported with an argon stream into inductively coupled argon plasma, where it is ionized. Various laser ablation systems suitable for LA-ICPMS are commercially available, mostly equipped with a Nd:YAG laser (e.g., from New Wave, Fremont, CA, or from CETAC Technologies, Omaha, NE, working at wavelengths of 266 nm and mainly 213 nm). In LA-ICPMS, different types of mass spectrometers, mostly quadrupole-based inductively coupled plasma mass spectrometers or double-focusing sector field instruments, are utilized. Quadrupole mass spectrometers are very robust and stable over many hours, which is an important precondition for time-consuming imaging studies on biological tissues. More expensive ICP sector field mass spectrometers provide higher sensitivity and improved limits of detection at low mass resolution ($m/\Delta m \approx 300$). Advantages of LA-ICPMS are (a) the virtually simultaneous determination of most trace and minor elements in biological tissue, (b) the direct measurement of tissue sections (no additional sample preparation is required, and contamination chances are low), (c) low relative limits of detection (LODs; 0.001−1 μg g^{-1}), and (d) a lateral resolution of 5−200 μm. Furthermore, complete ablation of biological samples (with section thicknesses of <100 μm) on glass substrates is possible, thus eliminating fractionation effects during the laser ablation process. Analytical data are easy to quantify if homogeneous matrix-matched standards are available with the precision of trace metal distribution ranging between 5% and 10%. Major limits of LA-ICPMS are isobaric interferences by analyte atomic ions (e.g., $^{40}Ca^+$ and $^{40}Ar^+$) and by polyatomic ions (e.g., $^{41}K^+$ and $^{40}ArH^+$) at the same nominal mass. However, for example, iron can be measured in biological tissue sections by LA-ICPMS at m/z 56 due to a constant background formed by ArO^+ ions which can be subtracted. As no suitable certified reference material for quantification of LA-ICPMS is available, different reliable quantification strategies for the LA-ICPMS data using homogeneous matrix-matched laboratory standards or solution-based calibration for bioimaging of metals in tissues have been established and employed.

By using LA-ICPMS, in our BrainMet (Bioimaging of Metals in Brain and Metallomics) laboratory at Forschungszentrum Jülich, we have systematically investigated the metal distribution in brain using human and rodent samples under physiological and pathological conditions.[2,3,29,30] All these investigations on tissue sections demonstrated that the LA-ICPMS imaging technique developed can produce valid and statistically robust quantitative results in these biological samples. Therefore, it is promising to extend this analytical technique to other biological tissues.

Metals such as Cu, Zn, and Fe at trace concentration levels are essential components for life and play a key role in cellular and molecular processes of biological systems.[31−34] In the pathogenesis of coronary heart disease (CHD) profound changes of metal concentrations occur in the realm of inflammatory infiltration of the intima, plaque formation, and remodeling of the arterial smooth muscle layer. Changes in the metal inventory were also described in myocardial tissue suffering from intermittent shortenings of blood supply by affected vessels. Finally, differences in systemic metal content in patients affected by coronary heart disease compared to controls have been described and may result from the inflammatory component of systemic arteriosclerosis or from cardiac insufficiency or constitute a trait marker somehow related to an increased coronary risk.[35]

Trace metal concentrations in heart tissue and the correlation to the pathogenesis of heart diseases have been studied after digestion of sample material using various conventional trace analytical techniques, such as ICP-OES (inductively coupled plasma optical emission spectrometry), ICPMS (inductively coupled plasma mass spectrometry), or AAS (atomic absorption spectrometry).[35] These studies suggested that the development of certain heart diseases may be associated with concentration changes of some biometals. For example, Altekin et al. demonstrated increased serum copper and iron levels and decreased selenium and zinc levels in patients with myocardial infarction.[36] In an epidemiological study in eastern Finland Salonen and co-workers[37] observed an elevated copper concentration in serum as an independent risk factor for ischemic heart disease. Serum copper concentrations at 1 μg mL^{-1} or more were associated with a 3.5-fold risk of acute myocardial infarction.[37]

Following myocardial infarction, it can be expected that due to the demise of tissue and as a function of its extent intracellular metals will be liberated while later acute-phase and remodeling processes may consume certain metals. Clinical studies revealed that serum copper levels in patients with myocardial infarction

(21) McDonnell, L.; Heeren, R. M. A.; de Lange, R. P. J.; Fletcher, I. W. *J. Am. Soc. Mass Spectrom.* **2006**, *17*, 1195.
(22) Smart, K. E.; Kilburn, M. R.; Salter, C. J.; Smith, J. A. C.; Grovenor, C. R. M. *Int. J. Mass Spectrom.* **2007**, *260*, 107.
(23) Guerquin-Kern, J. L.; Wu, T. D.; Quintana, C.; Croisy, A. *Biochim. Biophys. Acta, Gen. Subj.* **2005**, *1724*, 228.
(24) Walker, A. V. *Anal. Chem.* **2008**, *80*, 8865.
(25) Heeren, M. A.; Mc.Donnell, L. A.; Amstalden, E.; Luxambourgh, S. L.; Altelaar, A. F. M.; Piersma, S. R. *Appl. Surf. Sci.* **2006**, *252*, 6827.
(26) Chandra, S.; Tjarks, W.; Lorey, D. R.; Barth, R. F. *J. Microsc.* **2007**, *229*, 92.
(27) Jones, E. A.; Lockyer, N. P.; Vickerman, J. C. *Int. J. Mass Spectrom.* **2007**, *260*, 146.
(28) McDonnell, L. A.; Heeren, R. M. A. *Mass Spectrom. Rev.* **2007**, *26*, 606.
(29) Zoriy, M.; Dehnhardt, M.; Matusch, A.; Becker, J. S. *Spectrochim. Acta, B* **2008**, *63*, 375.
(30) Becker, J. S.; Zoriy, M.; Pickhardt, C.; Palomero-Gallagher, N.; Zilles, K. *Anal. Chem.* **2005**, *77*, 3208.
(31) Szpunar, J.; Lobinski, R.; Prange, A. *Appl. Spectrosc.* **2003**, *57*, 102A.
(32) Mertz, W. *Science* **1981**, *213*, 1332.
(33) Sigel, A.; Sigel, H.; Sigel, R. K. O. *Neurodegenerative Diseases and Metal Ions*; John Wiley & Sons, Ltd.: Chichester, U.K., 2006.
(34) Szpunar, J. *Anal. Bioanal. Chem.* **2004**, *378*, 54.
(35) Manthey, J.; Stoeppler, M.; Morgenstern, W.; Nussel, E.; Opherk, D.; Weintraut, A.; Wesch, H.; Kubler, W. *Circulation* **1991**, *64*, 722.
(36) Altekin, E.; Coker, C.; Sişman, A. R.; Onvural, B.; Kuralay, F.; Kirimli, O. *J. Trace Elem. Med. Biol.* **2005**, *18*, 235.
(37) Salonen, J. T.; Salonen, T.; Korpela, H.; Suntioinen, S.; Tuomilehto, J. *Am. J. Epidemiol.* **1991**, *134*, 268.

were significantly higher for the patients with a complicated course versus patients with an uncomplicated course.[38] A significant correlation of serum copper and the markers of cardiac infarction, creatinine phosphokinase and lactic dehydrogenase, was found. Serial assessment of Cu and Zn serum levels following acute myocardial infarction until day 10 following the attack showed a significant rise of Cu ($p < 0.01$) after day 5, peaking between day 7 and day 10. Zn decreased significantly ($p < 0.01$) with respect to that of the control group from the first day on, with the lowest values at day 3.

For a better interpretation of such data it should be kept in mind that the total content of a metal is distributed over a free compartment and protein-bound compartments. The affinity and stability of the metal binding can be very variable from protein to protein. Accordingly, only about 0.1% of Cu occurs free, and thus, the total serum Cu showed a remarkable correlation with the albumin-bound and globulin-bound Cu (ceruloplasmin), as well as with the total concentrations of these protein fractions. In other words, the total serum Cu largely depends on the availability of carrier proteins. In contrast, the total serum Zn only depended on the albumin concentration, but not on that of globulins.[39] Recently, the kinetics of the exchange of zinc by copper within the binding to bovine serum albumin was studied by Becker et al. using an isotopically enriched copper tracer (^{65}Cu), separation by one-dimensional gel electrophoresis, and analysis by LA-ICPMS.[40] These isotope ratio measurements suggested an exchange of Zn by Cu on bovine serum albumin within a few minutes.

Moreover, analysis of biopsy material collected during bypass surgery evidenced significant correlations of cardiac output and myocardial selenium, iron, copper, zinc, and phosphorus.[41] Thus, it is of interest to further determine metal distributions in diseased heart tissue in comparison to controls.

The aim of this work was to study the feasibility of LA-ICPMS imaging to analyze metal distributions in mouse heart sections. Moreover, SIMS using a pulsed primary Bi cluster (Bi_n^+) ion source as imaging technique will be developed to detect metals and small biomolecules in mouse heart. The synergy of both imaging mass spectrometric techniques will be discussed.

EXPERIMENTAL SECTION

LA-ICPMS: Instrumentation and Measurements. A commercial laser ablation (LA) system (New Wave UP 266, Fremont, CA) was coupled to a quadrupole inductively coupled plasma mass spectrometer (XSeries2, Thermo Fisher Scientific, Germany) to accomplish elemental imaging in heart tissues. The laser ablation system was operated with a frequency-quadrupled Nd:YAG laser (wavelength of 266 nm, repetition frequency of 20 Hz, and spot diameter of 160 μm). Argon was used as the carrier gas that transported the ablated material into the ICP. The ions formed in the ICP were separated according to their mass-to-charge ratio. The maximum ion intensity was observed at a carrier gas flow rate of 0.86 L min^{-1}. The distribution of metals in sections of heart tissue was investigated by LA-ICPMS under the optimized experimental parameters as summarized in Table S1 (Supporting Information). The heart sample and matrix-matched standards were arranged in a laser ablation chamber to allow imaging LA-ICPMS analysis under identical experimental conditions.

SIMS: Instrumentation and Measurements. The SIMS measurements were carried out using a commercial time-of flight mass spectrometer: ToF-SIMS IV from IONTOF GmbH, Münster, Germany. The instrument was equipped with a pulsed primary Bi cluster (Bi_n^+) ion source running at 25 keV. The primary ion pulses were bunched to 1 ns, which gives a mass resolution of about 8000 ($m/\Delta m$) at m/z 30. This is sufficient to resolve interferences of the elemental ions from molecules with the same nominal mass. The ion pulse repetition rate was 10 kHz, and this corresponds to an accessible mass of up to m/z 800.

Due to the acceptance of the mass spectrometer SIMS imaging is limited to a maximum sample area of 500 μm × 500 μm. In combination with a stage raster imaging of larger sample areas, such as 16 mm × 9 mm (for mouse heart sections), is possible. For each shot a complete mass spectrum was acquired and stored. We chose a pixel distance of 33 μm and applied 150 shots to each pixel. The lateral resolution is limited by the pixel distance and not by the primary ion beam diameter. The number of shots enabled a dynamic range of 2 orders of magnitude in the images. A mapping at these parameters is completed within less than 1 h. Because the tissue sample was mounted on a glass substrate, electron flooding was applied for charge compensation. As an advantage of SIMS imaging the sample is not damaged due to the low ion dose applied and can be used for further investigations. The optimized experimental parameters for SIMS imaging are summarized in Table S1b (Supporting Information). Because the complete mass spectra are stored during the SIMS measurements, the images of the ions of interest can be reconstructed retrospectively.

Samples, Sample Preparation, and LA-ICPMS Standards. All heart samples were isolated from healthy male mice, six months of age, dissected, embedded in Tissue-Tec OCT, quick frozen in liquid nitrogen, and then stored in a −80 °C freezer. Sections were cut on a cryostat at a thickness of 14 μm for hematoxylin and eosin (HE) staining and 40 μm for LA-ICPMS and SIMS measurements. The native cryosections were directly mounted onto glass slides. Matrix-matched tissue standards with well-defined concentrations of the metals of interest were used for the calibration of analytical data in LA-ICPMS. The preparation of matrix-matched laboratory standards and the LA-ICPMS calibration procedure are described elsewhere.[3,30] During LA-ICPMS measurements the tissue section was systematically scanned (line by line) by a focused laser beam. From the continuous list of raw pixel values elemental images were reconstructed using LA-ICPMS Image Generation software created by the Juelich Research Centre. Metal concentrations were measured within freely drawn regions of interest (ROIs) onto parametric maps using PMOD version 3.0 (www.pmod.com). Adjacent sections were stained by HE to illustrate the structure of heart tissue.

RESULTS AND DISCUSSION

The entire analytical procedure from sample preparation by cryocutting of biological tissue via the LA-ICPMS bioimaging procedure, where the sample is scanned (line by line) by a focused laser beam and ion intensities of analytes of interest are measured,

(38) Singh, M. M.; Singh, R.; Khare, A.; Gupta, M. C.; Patney, N. L.; Jain, V. K.; Goyal, S. P.; Prakash, V.; Pandey, D. N. *Angiology* **1985**, *36*, 504.
(39) Jain, V. K.; Mohan, G. *Biol. Trace Elem. Res.* **1991**, *31*, 317.
(40) Becker, J. Su.; Pozebon, D.; Dressler, V. L.; Lobinski, R.; Becker, J. S. *J. Anal. At. Spectrom.* **2008**, *23*, 1076.
(41) Oster, O.; Dahm, M.; Oelert, H. *Eur. Heart J.* **1993**, *14*, 770.

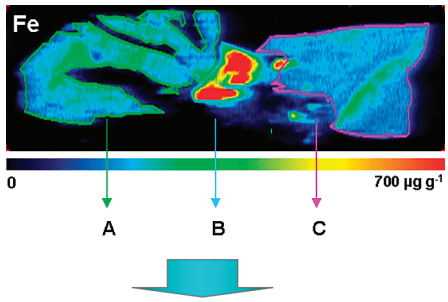

Fe distribution in heart tissue.

	Concentration, µg g^{-1}		
	Mean	Min.	Max.
A	125	45	340
B	358	138	711
C	139	62	247

Figure 1. Reconstructed iron image measured by LA-ICPMS. The included table summarizes iron concentrations determined in heart tissue (using PMOD).

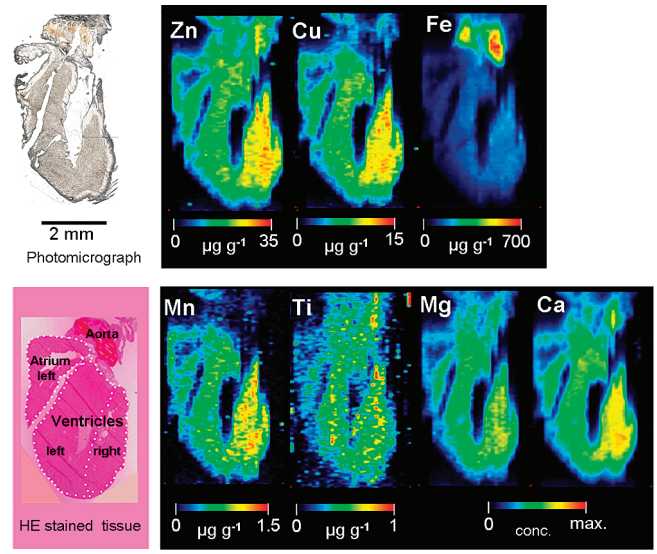

Figure 3. Elemental distribution (Zn, Cu, Fe, Mn, Ti, Mg, Ca, and S) in a 40 μm section of heart tissue analyzed by LA-ICPMS and photomicrographs of native and hematoxylin and eosin stained tissue.

up to a final evaluation of the data using the LA-ICPMS Image Generation software written in house, yielding quantitative images of metals, is described elsewhere by Becker et al.[2,4] Figure 1 shows the Fe distribution in a section through a swing-opened mouse heart within selected regions (aorta and ventricles) using PMOD. Quantitative images of the transition metals Zn, Cu, Fe, Mn, and Ti measured by LA-ICPMS are shown in Figure 2. In addition, noncalibrated distributions of alkaline-earth metals Mg and Ca are presented. The ion images of alkali metals $^{23}Na^+$ and $^{39}K^+$ and of nonmetals $^{31}P^+$, $^{12}C^+$, and $^{34}S^+$ obtained by LA-ICPMS are summarized in the upper row of Figure 3. The metal and nonmetal images show clearly the shape and the anatomy of the heart tissue investigated as shown in the photomicrographs of neighboring sections (left in Figure 2). All elements were inhomogeneously distributed. In this work, no quantification of alkali metals, alkaline-earth metals, and nonmetals was possible due to the lack of suitable reference material. Of the elements assessed here in terms of concentration, the highest regional metal concentration was observed for Fe (360 μg g^{-1} on average) in blood present in the lumen of the aorta. This value is in accordance with a literature value of 400 μg g^{-1} for mouse blood and largely due to hemoglobin-bound iron.[42] In the heart muscle tissue (myocardium) iron concentrations of about 130 μg g^{-1} occurred, which are high compared to those in other tissues such as brain (about 10 μg g^{-1}) and may largely be constituted by myoglobin-bound iron.

In comparison with the high Fe content, other metals occurred at lower concentrations and were enriched to a higher extent in the myocardium than in the blood. Zn reached a maximum concentration of 35 μg g^{-1} and Cu 15 μg g^{-1} in the myocardium. Ti and Mn were found at lower concentrations (up to 1 and 1.5 μg g^{-1}, respectively). Locally high signals for carbon (see Figure 3) and in close correlation for phosphorus corresponded to regions with lower water content, which was the case in the middle of the ventricle wall, where muscle fibers of several

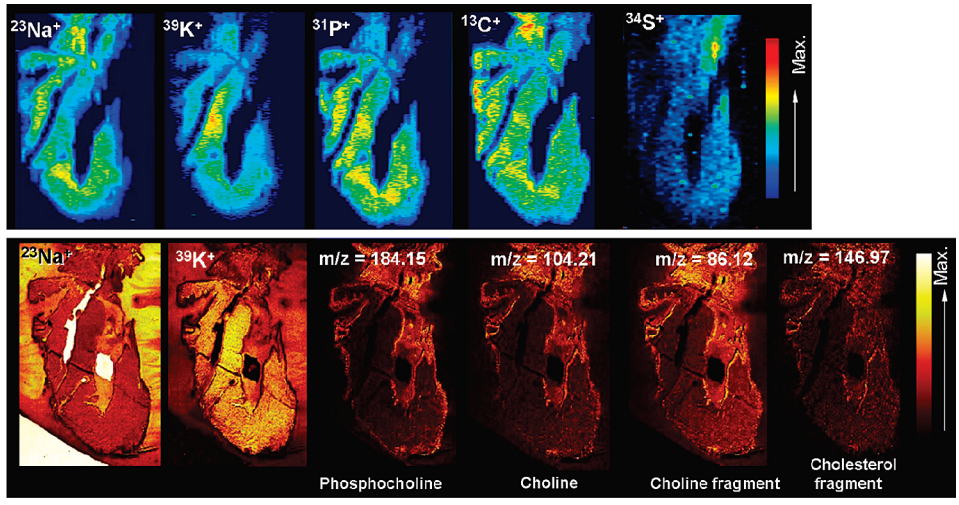

Figure 2. Ion images of a 40 μm section obtained by LA-ICPMS (rainbow scale) and SIMS (heat scale): LA-ICPMS images of the alkali metals $^{23}Na^+$ and $^{39}K^+$ and nonmetals $^{31}P^+$, $^{13}C^+$, and $^{34}S^+$ (upper row). SIMS images of alkali metals $^{23}Na^+$ and $^{39}K^+$ and biomolecules phosphocholine (*m*/*z* 184.14), choline (*m*/*z* 104.21) choline fragment (*m*/*z* 86.12), and cholesterol fragment (*m*/*z* 146.97) (lower row).

Table 1. Figures of Merit of LA-ICPMS and ToF-SIMS Imaging of Tissue

	LA-ICPMS	ToF-SIMS
application fields	parallel determination of trace, minor, and major elements in biological tissue, isotope ratios	parallel determination of elements and molecules in biological tissue, isotope ratios
sample type	thin native cryosections on glass substrate (laser ablated at atmospheric pressure)	thin native cryosections on glass substrate (vacuum compatible, UHV ion source 5×10^{-10} mbar)
sample size (max)	100 mm × 100 mm (complete ablation of tissue)	70 mm × 100 mm (nearly no sample consumption)
sample preparation	no	no
mass range	6−250 Da	1−2000 Da
mass resolution ($m/\Delta m$)	ICP-QMS, 300; ICP-SFMS, 300, 3000, 12000[a]	<10000
information depth	thickness of section, <100 μm	few atomic layers on the top
spatial resolution	5−120 μm	$m/\Delta m$ − 300, sub-micrometer; $m/\Delta m$ − 8000, 1−3 μm
LODs	0.001−1 μg g^{-1}	large scatter, in favorable cases to μg g^{-1}
fraction effects	no	reduced by Bi_3^+ cluster ion bombardment
matrix effects	less than 1 order of magnitude	large scatter of RSF[b] up to 5 orders of magnitude
quantification of images	easy; needs homogeneous reference materials	very difficult due to large matrix effects
precision of metal distribution	5−10%	
isobaric interferences	resolved by collision cell ICPMS (or ICP-SFMS)	resolved at high mass resolution
measurement time	4 h/cm^2	0.5 h/cm^2
software	house-written Image Generation software	SurfaceLab 6
imaging generation	preselected masses defined before imaging	definition of peak lists during and after the data acquisition; retrospective image analysis

[a] ICP-QMS = quadrupole-based ICPMS; ICP-SFMS = sector field ICPMS. [b] RSF = relative sensitivity factor. [c] Depending on the size, required spatial resolution, and required dynamic range.

directions cross, whereas at the inner and outer surfaces fibers tend to be more parallel.

Indeed, the present data suggest higher concentrations of Zn, Mn, Cu, Mg, and Ca measured by LA-ICPMS in the right ventricle compared to the left ventricle. An artifact due to higher slice thickness in this area can be eliminated as differences in slice thickness should also be reflected by P, C, Na, and K, which here even tended to be lower in the right ventricle. One explanation for lower Zn, Mn, Cu, Mg, and Ca in the left ventricle could be the higher metabolic turnover there as it has to pump against a 4−6-fold higher pressure than the right ventricle.

In addition to LA-ICPMS imaging, SIMS as an elemental and biomolecular mass spectrometric technique was employed for imaging of Na and K. A clear contamination of both these alkali metals surrounding the tissue on the glass substrate in SIMS images is visible. In SIMS only a few atomic layers were sputtered by the primary bismuth cluster ion beam. Therefore, the images generated represent the upper nanometers at the sample surface and not averages across the entire sample cross section as is the case in LA-ICPMS, which completely ablates the 40 μm sample thickness. In our example, vertical transport of Na and K to the upper surface of the embedding medium during drying may have accounted for the high SIMS signal there. In contrast, lateral transport of highly soluble Na and K toward the last drop during drying is likely to account for an enrichment of Na and K in the center of the sample compared to the rim. Freeze-drying may reduce these effects. Notwithstanding and congruent in LA-ICPMS and SIMS, Na and K showed in parts a mutually complementary distribution in the present section. This is likely in relation to the intra/extracellular K/Na gradient. As can be seen from the microphotograph, in agreement with the intracellular enrichment of K, higher K occurred in an area where fibers are most densely packed which thus contains a higher fraction of intracellular space and vice versa for Na.

Under the experimental conditions used for SIMS measurements K and Na were detected with very high ion intensities in heart tissue. This may be caused not only by their high abundance (literature values about 3000 μg g^{-1} K and 700 μg g^{-1} Na in meat) but also by their preferential detectability due to a low first ionization energy (4.3 eV (K) and 5.1 eV (Na)).

Other analytes detected by SIMS were also comparatively abundant. Concentrations of total choline of about 1200 μg g^{-1} and cholesterol of about 1500 μg g^{-1} in meat were reported in the literature.[43] Not enough material is sputtered to detect other metals at a lower concentration level (such as Ca, Mg, Fe, Cu, Zn, Mn, and Ti).

A comparison of the figures of merit with respect to the application fields, sample type, size, and preparation, mass range and resolution, information depth, spatial resolution and LODs, fractionation and matrix effects, quantification possibilities, precision of metal distribution, measurement time, and software of the LA-ICPMS and SIMS techniques is given in Table 1. Both imaging techniques have advantages over MALDI-MS imaging: (a) no sample preparation is required, (b) native biological tissue can be measured directly, and (c) no matrix application is required as in MALDI-MS. SIMS using a Bi cluster (Bi_n^+) ion source produces secondary ions of atoms and molecules with increasing secondary ion yield and decreasing sample damage (therefore, SIMS and LA-ICPMS imaging can be performed on one tissue slice).

In general, SIMS and LA-ICPMS as spatially resolved imaging techniques yield similar element distributions. SIMS measurements are possible at significantly higher lateral resolution (submicrometer) compared to those of LA-ICPMS (>5 μm). Within the heart area images of Na and K were congruent in LA-ICPMS and SIMS. The phosphorus image measured by LA-ICPMS may share features of the phosphocholine distribution obtained with SIMS measurements at m/z 184.15. In addition, choline at m/z 104.21, a choline fragment at m/z 84.12, and a cholesterol fragment at m/z 146.97 were detected by SIMS. The 2D images of these

(42) Modi, M.; Flora, S. J. *Cell Biol. Toxicol.* **2007**, *23*, 429.
(43) Nutrient Data Laboratory, National Agricultural Library, United States Department of Agriculture. http://fnic.nal.usda.gov/nal_display/index.php?info_center=4&tax_level=1.

biomolecules measured by SIMS and of nonmetals analyzed by LA-ICPMS are summarized in Figure 3. The concentration of these lipids was clearly highest in the endocardium, imposing as a continuous line and in discontinuous lines at the outer surface of the ventricles corresponding to larger coronary arteries. In pathological tissue such a combination of SIMS and LA-ICPMS would allow a correlation of cholesterol and lipids as markers and constituents of artherosclerotic plaques with metals altered due to the ischemic metabolic situation.

CONCLUSIONS

LA-ICPMS and SIMS are powerful imaging techniques to study elemental and molecular distributions in biological samples. As a first attempt, we developed imaging LA-ICPMS to determine and quantify the metal distribution in mouse heart. For the first time the elemental and biomolecular images of biological tissues obtained by two different mass spectrometric imaging techniques, LA-ICPMS and SIMS, were compared to gain novel information.

Our results suggest that LA-ICPMS and SIMS have great potential to image metals and biomolecules. The application of both LA-ICPMS and SIMS in the same section can provide insights into the synergy of metals and biomolecules.

ACKNOWLEDGMENT

J.S.B. thanks J. Srega and M. Hamester (Thermo Fisher Scientific, Bremen, Germany) for instrumental support of the BrainMet laboratory at the Research Centre Juelich.

SUPPORTING INFORMATION AVAILABLE

Additional information as noted in the text. This material is available free of charge via the Internet at http://pubs.acs.org.

Received for review August 27, 2010. Accepted October 11, 2010.

AC102256Q